Laminar Boundary Layer at an Infinite Swept Stagnation Line with Large Rates of Injection

PAUL A. LIBBY* AND DAVID R. KASSOY†
University of California at San Diego, La Jolla, Calif.

Earlier calculations of the effect of injection on the three-dimensional boundary layer along an infinite, swept stagnation line have been extended to the "massive blowing" situation. Numerical results relative to boundary-layer properties for large injection are supplemented by an asymptotic analysis reflecting the inner layer and free mixing structure of such flows. The density ratio relating the density in the inner layer to that in the external stream is found to play a crucial role in determining the nature of the boundary layer. Separation of the spanwise flow is found to occur while the chordwise flow experiences finite wall shear for all finite rates of injection provided the wall density is finite.

Nomenclature

f = stream function for streamwise velocity component
$\bar{f}$ = stretched stream function, $f\epsilon$
h = static enthalpy
h_s = stagnation enthalpy
I_i = integral thicknesses for boundary layers [Eqs. (12)]
J_i = integral thickness for free-mixing layers [Eqs. (24)]
$\tilde{m}$ = streamwise Mach number parameter [Eq. (11)]
u = chordwise velocity component
v = streamwise velocity component
w = normal velocity component
x = chordwise coordinate
y = streamwise coordinate
z = normal coordinate
α = chordwise velocity gradient, $(du_e/dx)_{x=0}$
γ,ω = parameters in density ratio [Eq. (11)]
ϵ = expansion parameter, $-\varphi_w^{-1}$
η = transformed normal coordinate [Eq. (5)]
$\bar{\eta}$ = transformed normal coordinate, $\eta\epsilon$
$\hat{\eta}$ = transformed normal coordinate, $\eta - \lambda(\epsilon)$
λ = parameter in translational transformation [Eq. (19)]

Subscripts

e = conditions in external stream
o = defining edge of inner layer
s = stagnation conditions
s,e = stagnation conditions in external stream

1 Introduction

IN two circumstances it is possible for the boundary layer to involve large rates of mass transfer: when radiative heat transfer is so large as to uncouple effectively the mass transfer from the convective heat transfer on an ablating surface and when the rate at which a coolant is injected through a porous surface is determined by other than local considerations, e.g., by conditions downstream of that surface. Because of the technological interest in these circumstances there have been several studies of boundary layers with large rates of mass transfer. References 1–5 are representative. In the present work we are concerned with a three-dimensional example of such a flow.

Received September 26, 1969; revision received April 14, 1970. The research reported here was carried out as part of the program supported by the NASA under Grant NGR-05-009-025. The authors gratefully acknowledge the assistance of P. Wu in carrying out the numerical calculations and the criticism of an anonymous reviewer regarding our original translational transformation, Eq. (19); this criticism lead to the correct version given here.

* Professor of Aerospace Engineering. Fellow AIAA.
† Assistant Professor of Aerospace Engineering. Member AIAA.

Consider the boundary layer along an infinite, swept stagnation line with mass transfer. We remark that this flow is one in which the distribution of mass transfer assumed for analytic convenience is actually realistic, namely, uniform, i.e., $(\rho w)_w$ = constant. Although several investigators have treated various aspects of this flow, Beckwith[6] provides the work most relevant for our purposes since he considers injection but at rates small in terms of our present interest. Accordingly, we extend his numerical results to large rates of injection.

When boundary layers are subjected to large rates of mass transfer, the boundary-layer thickness in terms of the usual transformed normal coordinates becomes large, although in tersm of physical coordinates it will remain small for a suitably large Reynolds number. Moreover, within this thickness such boundary layers have a structure characterized by an inner layer which is close to the surface and in which the injected fluid plays dominant roles and by an outer, relatively thin layer which adjusts the inner layers to the external flow. In the inner layer shear forces are negligible and pressure and inertia forces predominant, whereas in the outer layer all forces are important.

The structure of boundary layers subject to large rates of injection results in difficulties in numerical calculations. Large ranges of the independent variable related to the normal coordinate are required. In addition the two-point boundary conditions require in general either iteration or trial and error for the determination of the crucial wall values; for large rates of injection these wall values are small and convergence is poor. Thus it is convenient to have an approximate analysis for large rates of injection reflecting the structure of such boundary layers. Accordingly we follow the spirit of Kubota and Fernandez,[5] provide for this three-dimensional case such an approximate solution using the method of matched asymptotic expansions, and compare our numerical results therewith as the rate of injection increases.

2 Analysis

Figure 1 shows schematically the flow under consideration. For a stagnation line of infinite extent in a fluid with unity Prandtl number the describing equations are

$$\rho w\, \partial v/\partial z = (\partial/\partial z)[\mu(\partial v/\partial z)] \tag{1}$$

$$\rho u(\partial u/\partial x) + \rho w(\partial u/\partial z) = \rho_s u_e(du_e/dx) + (\partial/\partial z)[\mu(\partial u/\partial z)] \tag{2}$$

$$\rho w(\partial h_s/\partial z) = (\partial/\partial z)[\mu(\partial h_s/\partial z)] \tag{3}$$

$$(\partial/\partial x)(\rho u) + (\partial/\partial z)(\rho w) = 0 \quad (4)$$

where all quantities are defined in a standard way and where for a stagnation line $(du_e/dx) = \text{constant} = \alpha$.

We now sketch the standard means for putting Eqs. (1–4) into similarity form. First introduce a new independent variable

$$\eta = [\rho_e\alpha/\mu_e]^{1/2}\int_0^z (\rho/\rho_e)dz' = \eta(z) \quad (5)$$

and let

$$v = v_e f'(\eta), \quad u = u_e\varphi'(\eta) = \alpha x\varphi'(\eta) \quad (6)$$

where $(\ )'$ denotes differentiation with respect to η.‡ Then Eq. (4) yields immediately the third velocity component

$$-\rho w = (\rho_e\mu_e\alpha)\varphi^{1/2} + \text{const} \quad (7)$$

We select the constant so that

$$\varphi(\eta = 0) = \varphi_w = -(\rho w)_w(\rho_e\mu_e\alpha)^{1/2} \quad (8)$$

Equations (1) and (2) then yield

$$f'''(\eta) + \varphi f'' = 0 \quad (9)$$

$$\varphi'''(\eta) + \varphi\varphi'' + [(\rho_e/\rho) - \varphi'^2] = 0 \quad (10)$$

provided $\rho\mu = \rho_e\mu_e$, a commonly made approximation.

We must now provide an expression for ρ_e/ρ; comparison of Eqs. (1) and (3) and the nature of a stagnation line suggest that a Crocco relation $h_s = A + Bv$ applies. This plus the approximate equation of state, $\rho^{-1} \propto h \equiv h_s - v^2/2$ leads to

$$\rho_e/\rho = \gamma^2(1 - f') + \omega f'(1 - f') + f'^2 \quad (11)$$

where $\gamma^2 \equiv g_w(1 - \tilde{m})^{-1}$, $\omega \equiv (1 - \tilde{m})^{-1}$, where $g_w = h_w/h_{s,e}$ and where $\tilde{m} \equiv v_e^2/2h_{s,e}$ is a combined Mach number-sweep parameter: $0 \leq \tilde{m} < 1$. Note that $\gamma, \omega \geq 0$.

The boundary conditions for Eqs. (9) and (10) with Eq. (8) taken into account are

$$\varphi(\eta = 0) = \varphi_w, \quad f'(0) = \varphi'(0) = 0, \quad f'(\infty) = \varphi'(\infty) = 1$$

We thus see that solutions are defined by the parameters γ, ω, and φ_w.

Equations (9–11) are essentially those solved by Beckwith[6] for injection, i.e., for $\varphi_w = 0, -0.5, -1.0$.§ Since we are interested in large rates of mass transfer we shall find numerical solutions for $-\varphi_w \gg 1$.

Of applied interest from the solutions of Eqs. (9–11) are the two skin-friction coefficients corresponding to the chordwise and spanwise shear stresses, the heat transfer, and certain integral thicknesses. The former quantities are readily related to $f''(0)$, $\varphi''(0)$; the integral thickness of interest can be established by performing the usual integrations with respect to z from 0 to ∞ on Eqs. (1) and (2) and be found to be related to

$$I_1 \equiv \int_0^\infty \varphi'(1 - \varphi')d\eta, \quad I_2 \equiv \int_0^\infty [(\rho_e/\rho) - \varphi']d\eta \quad (12)$$

We thus give results in terms of these four quantities.

Asymptotic Analysis

Equations (9–11) can be solved by numerical means for a range of parameters γ, ω, and φ_w. Before discussing the numerical analysis and the results thereof we turn to an approximate solution appropriate for $(-\rho w)$ large and let a small parameter be $\epsilon \equiv (-\varphi_w)^{-1}$. We follow the technique of Kassoy[4] and consider the original equations with η as the independent variable rather than employ a von Mises transformation as is done by Kubota and Fernandez.[5]

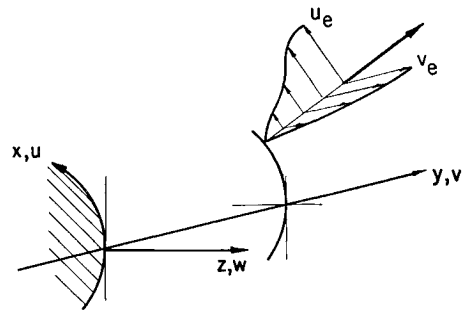

Fig. 1 Schematic representation of the flow.

The two-layer structure of the boundary layer with large rates of mass transfer suggests a rescaling of the independent variable by introduction of $\tilde{\eta} \equiv \epsilon\eta$ and changes in the dependent variables by introduction of $\tilde{\varphi} \equiv \epsilon\varphi$, $\tilde{f} = \epsilon f$. Eqs. (9) and (10) become

$$\epsilon^2\tilde{f}'''(\tilde{\eta}) + \tilde{\varphi}\tilde{f}'' = 0 \quad (9a)$$

$$\epsilon^2\tilde{\varphi}'''(\tilde{\eta}) + \tilde{\varphi}\tilde{\varphi}'' + [(\rho_e/\rho) - \tilde{\varphi}'^2] = 0 \quad (10a)$$

where $(\ )'$ now denotes differentiation with respect to $\tilde{\eta}$. The boundary conditions for these equations are $\tilde{f}(0) = \tilde{f}'(0) = \tilde{\varphi}'(0) = 0$ and $-\tilde{\varphi}(0) = \tilde{f}'(\infty) = \tilde{\varphi}'(\infty) = 1$.

Although these equations may be more suitable in some cases for numerical analysis for $-\varphi_w \gg 1$, $\epsilon \ll 1$ than the original set since the range of the independent variable is reduced, they are principally of use in obtaining approximate asymptotic solutions; from Eq. (9a) we can see that $\tilde{f}$ considered as a function of $\tilde{\eta}$ and satisfying the requirement $\tilde{f}(0) = 0$ is zero to all orders in a series expansion in ϵ. This implies that for large rates of injection the spanwise shear and the heat transfer, depending as they do only on $\tilde{f}'$, become zero, i.e., with respect to the spanwise boundary-layer separation occurs. However, we shall see below that the chordwise shear remains finite for all finite rates of injection, provided the wall temperature is nonzero, and thus that the surface streamlines become orthogonal to the stagnation line as the injection rate increases. These remarks concerning $\tilde{f}$ apply provided $\tilde{\varphi}(\tilde{\eta})$ is not zero; if $\tilde{\varphi}(\tilde{\eta}) = 0$, then $f''(\tilde{\eta})$ need not be zero. We thus expect that the value of $\tilde{\eta}$ at which $\tilde{\varphi}(\tilde{\eta}) = 0$ is special and that the outer layer wherein $f(\tilde{\eta}) \neq 0$ will be centered there. We denote this value of $\tilde{\eta} = \tilde{\eta}_0$.

We now confine our attention to Eq. (10a); if we assume a series in ϵ^2, i.e., $\tilde{\varphi}(\tilde{\eta};\epsilon) \simeq \tilde{\varphi}_0(\tilde{\eta}) + \epsilon^2\tilde{\varphi}_2(\tilde{\eta}) + \ldots$ we see that the equation for the zero-order term is

$$\tilde{\varphi}_0\tilde{\varphi}_0''(\tilde{\eta}) - \tilde{\varphi}_0'^2 = -\gamma^2 \quad (13)$$

Note that the shear stress term is of lower order in accordance with our previous remarks. We apply the two obvious boundary conditions at $\tilde{\eta} = 0$, i.e.,

$$\tilde{\varphi}_0(0) = -1, \quad \tilde{\varphi}_0'(0) = 0 \quad (14)$$

but must accept whatever behavior at $\tilde{\eta} > 0$ is forthcoming.

The solution for $\tilde{\varphi}_0$ is

$$\tilde{\varphi}_0 = -\cos\gamma\tilde{\eta} \quad (15)$$

which gives

$$\tilde{\varphi}_0'(\tilde{\eta}) = \gamma\sin\gamma\tilde{\eta}, \quad \tilde{\varphi}_0''(\tilde{\eta}) = \gamma^2\cos\gamma\tilde{\eta} \quad (16)$$

Thus we see that the crudest prediction of the behavior of the

‡ Because in the course of this analysis at least three independent variables η, $\tilde{\eta}$, $\hat{\eta}$, will appear, we shall be explicit as to such variables whenever confusion may arise.

§ The identification of our variables with those of Beckwith is obvious; in particular, $\tilde{m} \to 1 - t_s g_w \to t_w$. Therefore $\gamma^2 \to t_w/t_{s,} = t_w\lambda$, $\omega \to \lambda$. The reader may refer to Beckwith for relations giving γ^2 and ω in terms of freestream. Mach number and sweep angle for the special case of a thermally and calorically perfect gas.

chordwise wall shear with injection rate is

$$\varphi''(\eta = 0) = \varphi_w''(\eta) \simeq \gamma^2(-\varphi_w)^{-1} \tag{17}$$

For their $\beta = 1$ and our $\tilde{m} = 0$ this result agrees with Kubota and Fernandez.[5]

We now make several remarks concerning Eq. (17); first it can be established directly from Eq. (13) without finding the explicit solution for $\tilde{\varphi}_0(\tilde{\eta})$. Similarly, we can find $\tilde{\varphi}_2''(0)$, $\tilde{\varphi}_4''(0)$ without actually solving for $\tilde{\varphi}_2(\tilde{\eta})$ and $\tilde{\varphi}_4(\tilde{\eta})$ and indeed they turn out to be zero. Thus our crudest prediction for the chordwise shear parameter is correct through ϵ^4. We see from Eq. (17) and from the definition of γ that for a given injection rate in terms of φ_w and a given wall temperature in terms of g_w increasing sweep increases the chordwise shear and that for given φ_w and $\tilde{m}$ an increase in wall temperature likewise increases the chordwise shear. Finally, we note the key role of g_w in determining the behavior of the boundary layer near the surface; in particular $\varphi''(0)$ goes to zero as g_w goes to zero, all other parameters being fixed. We shall see that as $g_w \to 0$ the extent of the inner layer increases indefinitely.

The basic inner solution represented by $\tilde{f} \equiv 0$, and by Eq. (15) is a valid representation of the flow for $\tilde{\varphi}_0 \neq 0$. Equation (15) implies then that the inner region is restricted to the range

$$0 \leq \tilde{\eta} \leq \tilde{\eta}_0 = \pi/2\gamma \tag{18}$$

for at the upper bound of $\tilde{\eta}$, $\tilde{\varphi}(\tilde{\eta}_0) = 0$. In addition, $\tilde{\varphi}'(\tilde{\eta}_0) = \gamma$ where, in general, $\gamma \neq 1$, so that our inner solution does not satisfy the boundary conditions at $\eta \to \infty$ for either the spanwise or the chordwise boundary layer and we seek an outer solution permitting us to do so. In terms of our original dependent variable the outer edge of our inner layer is denoted by η_0 and is defined by $\eta_0 = \tilde{\eta}_0/\epsilon = \pi/2\gamma\epsilon$. Our outer layer is to be centered about this value. A translational transformation is clearly indicated; let

$$\hat{\eta} = \eta - \lambda(\epsilon) \tag{19}$$

such that

$$\lambda(\epsilon) = (\tilde{\eta}_0/\epsilon) + \lambda_1 + \sum_{n=2} \lambda_n/(\epsilon), \lambda_1 = 0(1), \lim_{\epsilon \to 0} (\lambda_{n+1}/\lambda_n) = 0,$$

$n > 1$ where all λ_n's must be found in the process of analysis. Since $\tilde{\eta} = \epsilon\eta$, the transformation may also be written as

$$\hat{\eta} = (\tilde{\eta} - \tilde{\eta}_0)\epsilon^{-1} - \lambda_1 - \sum_{n=2} \lambda_n(\epsilon)$$

It is to be noted that application of the inner limit $\epsilon \to 0$, $\tilde{\eta}$ less than $\tilde{\eta}_0$ and fixed, implies that the matching condition for the mixing layer is prescribed for $\hat{\eta} \to -\infty$.

Equations (9) and (10), invariant under the translational transformation in Eq. (19), describe the mixing layer in terms of the dependent variables $f = \hat{f}(\hat{\eta})$, and $\hat{\varphi} = \varphi(\hat{\eta})$. The external boundary conditions are simply

$$\lim_{\hat{\eta} \to \infty} \varphi'(\hat{\eta}), \hat{f}'(\hat{\eta}) = 1$$

The wall boundary conditions are replaced by the formal matching conditions

$$\lim_{\hat{\eta} \to -\infty} \{\epsilon\varphi(\hat{\eta}) - \tilde{\varphi}(\tilde{\eta} = \epsilon[\hat{\eta} + \lambda(\epsilon)])\} = 0$$

$$\lim_{\tilde{\eta} \to -\infty} \{\epsilon\hat{f}(\hat{\eta}) - \tilde{f}\} = 0$$

which produce the basic conditions

$$\begin{gathered} \hat{\varphi}(\hat{\eta} \to -\infty) = \gamma(\hat{\eta} + \lambda_1) \\ \hat{f}(\hat{\eta} \to -\infty) \times 0 \\ \hat{\varphi}'(\hat{\eta} \to -\infty) = \gamma \end{gathered} \tag{20a}$$

The third boundary condition for the $\hat{\varphi}$ equation

$$\varphi(\hat{\eta} = 0) = 0 \tag{20b}$$

derived by using the Prandtl transposition theorem in Eqs. (1–4) in a manner similar to that of Kassoy,[4] represents the location of the dividing streamline; i.e., $\eta_0 = \lambda(\epsilon)$.

Equations (9–11) subject to these boundary conditions yield three-dimensional free-mixing solutions, and the value of the constant λ_1. The external flow corresponding to $\eta \to -\infty$ is the usual one for a swept stagnation line. The inner flow, corresponding to $\hat{\eta} \to -\infty$, is one with zero spanwise velocity, with a constant density $\rho_{-\infty} = \rho_e/\gamma^2$ and with a maximum chordwise velocity equal to γu_e. Note that if $\gamma < 1$, i.e., if the inner flow is more dense than the external flow, then the chordwise velocity profiles associated with the free-mixing will have the usual shape with $\hat{\varphi}'(-\infty) < 1$, but that if $\gamma > 1$, the inner flow is less dense, $\hat{\varphi}'(-\infty) > 1$, and the chordwise velocity profile has velocity "overshoot." This result is analogous to the behavior at an axisymmetric stagnation point[7]; in both cases the chordwise velocity is dominated by the influence of pressure forces on the inner flow. The absence of spanwise forces in the inner layer results in the injected fluid moving only chordwise until it enters the outer viscous layer. As $\gamma \to 0$ the inner layer becomes infinitely dense, the chordwise pressure forces become ineffective, and the inner layer becomes stagnant and infinitely thick. In all of this we note the importance of the parameter γ. Note that the solutions for the outer layer depend only on two parameters γ and ω and not on φ_w itself.

We can construct from the previous first order inner and outer solutions a composite solution. For the velocity proves we obtain

$$\begin{aligned} \varphi'(\eta) &\simeq \gamma \sin(\gamma\eta\epsilon) + \hat{\varphi}'(\eta - \eta_0 - \lambda_1) - \gamma, \qquad 0 \leq \eta \leq \eta_0 \\ &\simeq \hat{\varphi}'(\eta - \eta_0 - \lambda_1), \quad \eta \geq \eta_0 \\ f'(\eta) &\simeq \hat{f}'(\eta - \eta_0 - \lambda_1) \end{aligned} \tag{21}$$

Equations (21) can be used to compute two term estimates for the integral quantities defined by Eqs. (13), namely

$$I_1 \simeq \epsilon^{-1}[1 - (\gamma\pi/4)] + \int_{-\infty}^{0} (\hat{\varphi}' - \gamma)(1 - \hat{\varphi}')d\hat{\eta} + \int_0^{\infty} \hat{\varphi}'(1 - \hat{\varphi}')d\hat{\eta} + \gamma\lambda_1 \tag{22}$$

$$I_2 \simeq \epsilon^{-1}[(\gamma\pi/2) - 1] + \int_{-\infty}^{0} [(\rho_e/\rho) - \gamma^2 - \hat{\varphi}' + \gamma]d\hat{\eta} + \int_0^{\infty} [(\rho_e/\rho) - \hat{\varphi}']d\hat{\eta} + \lambda_1\gamma(\gamma - 1)$$

The various integrals involving $\hat{f}(\hat{\eta})$ and $\hat{\varphi}(\hat{\eta})$ define integral thicknesses appropriate for free-mixing solutions. Accordingly, we present the numerical results therefor with the notation

$$\begin{aligned} J_1 &\equiv \int_{-\infty}^{0} (\hat{\varphi}' - \gamma)(1 - \hat{\varphi}')d\hat{\eta} \\ J_2 &\equiv \int_0^{\infty} \hat{\varphi}'(1 - \hat{\varphi}')d\hat{\eta} \\ J_3 &\equiv \int_{-\infty}^{0} [(\rho_e/\rho) - \gamma^2 - (\hat{\varphi}' - \gamma)]d\hat{\eta} \\ J_4 &= \int_0^{\infty} [(\rho_e/\rho) - \hat{\varphi}']d\hat{\eta} \end{aligned} \tag{23}$$

Numerical Analysis

We consider next the numerical analysis applicable to Eqs. (9–11). We apply the techniques of quasilinearization[8,9] in order to treat the problem of the two point boundary conditions. In the present case there is no question of uniqueness as $\eta \to \infty$ so that it is sufficient to impose "infinity" conditions at values of η, denoted η^*, sufficiently large so that $f'''(\eta^*)$, $\varphi''(\eta^*)$ are negligibly small. As $(-\varphi_w)$ increases, the required η^* increases. Our numerical results have been com-

Table 1 Properties of boundary-layer solutions

γ^2	ω	$-\varphi_w$	$f_w''(\eta)$	$\varphi_w''(\eta)$	I_1	I_2
0.3	0.15	0	0.5034	0.7007	0.4300	−0.1593
		0.5	0.2105	0.4285	0.5741	−0.2197
		1	0.0482	0.2669	0.7847	−0.3025
		1.5	0.0048	0.1908	1.0449	−0.3989
		2	0.0002	0.1474	1.3193	−0.4913
		2.5	0.0000	0.1191	1.5974	−0.5757
		3	0.0000	0.0996	1.8774	−0.6551
	3	0	0.5762	1.1273	0.2316	0.6641
		0.5	0.2907	0.7651	0.2721	0.7209
		1	0.0983	0.4444	0.3477	0.7490
		1.5	0.0139	0.2283	0.4975	0.7333
		2	0.0005	0.1493	0.7342	0.6809
		2.5	0.0000	0.1191	1.0044	0.6104
		3	0.0000	0.0996	1.2817	0.5361
	6	0	0.6290	1.5170	0.0239	1.4693
		0.5	0.3460	1.0866	−0.0198	1.6262
		1	0.1413	0.6624	−0.0465	1.7553
		1.5	0.0292	0.3134	−0.0057	1.8248
		2	0.0013	0.1557	0.1666	1.8226
		2.5	0.0000	0.1192	0.4237	1.7719
		3	0.0000	0.0996	8.6978	1.7040
3	1.5	0	0.6582	2.2500	0.0248	2.2004
		0.5	0.3942	2.0083	−0.0656	2.6395
		1	0.2059	1.7687	−0.1975	1.1637
		1.5	0.0903	1.5341	−0.3675	3.7692
		2	0.0320	1.3155	−0.5645	4.4446
		2.5	0.0088	1.1245	−0.7746	5.1738
		3	0.0018	0.9670	−0.9870	5.9410
		3.5	0.0003	0.8413	−1.1963	7.7339
		4	0.0000	0.7417	−1.4011	7.5439
		4.5	0.0000	0.6620	−1.6017	8.3654
		5	0.0000	0.5972	−1.7990	9.1952
	30	0	0.8803	4.8611	−1.7542	8.3696
		0.5	0.6054	4.1698	−2.2953	9.2607
		1	0.3793	3.4071	−2.8938	10.1949
		1.5	0.2068	2.6266	−3.5123	11.1514
		2	0.0909	1.9105	−4.0987	12.1081
		2.5	0.0287	1.3589	−4.5947	13.0486
		3	0.0060	1.0264	−4.9687	13.9642
		3.5	0.0009	0.8511	−5.2489	14.8491
		4	0.0001	0.7428	−5.4834	15.7100
		4.5	0.0000	0.6621	−5.6986	16.5595
		5	0.0000	0.5972	−5.9042	17.4059
	60	0	1.0061	7.1434	−3.3907	13.9251
		0.5	0.7287	6.1858	−4.2434	15.1731
		1	0.4917	5.1148	−5.1701	16.4557
		1.5	0.2993	3.9832	−6.1294	17.7426
		2	0.1550	2.8714	−7.0626	18.9973
		2.5	0.0613	1.8986	−7.8922	20.1837
		3	0.0154	1.2170	−8.5323	21.2825
		3.5	0.0022	0.8863	−8.9544	22.2961
		4	0.0002	0.7468	−9.2427	23.2330
		4.5	0.0000	0.6624	−9.4793	25.1218
		5	0.0000	0.5972	−9.6956	24.9892

pared to those of Beckwith[6] for unity Prandtl number and $\mu \propto T$ for several check cases and are found to agree to all significant figures available.

The success of quasilinearization for the present problem is found to depend on the size of η_0; for example, for $\gamma^2 = 0.3$ which results in $\eta_0 = 2.87(-\varphi_w)$, convergence of the iterative scheme is readily obtained until $-\varphi_w \simeq 3$. For greater values of $(-\varphi_w)$ successive iterates fail to converge for reasons to be discussed below. On the other hand, for $\gamma^2 = 3$, $\eta_0 = 0.91$ $(-\varphi_w)$ and the technique is successful to at least $-\varphi_w \simeq 5$, the largest value we have considered.

The reason for the difficulty may be seen from Eq. (10a) rewritten in the form

$$(\tilde{\varphi}''(\tilde{\eta}))' = -\epsilon^{-2}\{\tilde{\varphi}(\tilde{\varphi})'' + [(\rho_e/\rho) - \tilde{\varphi}'^2]\}$$

As $(-\varphi_w)$ increases, ϵ decreases; moreover, in the range $0 \leq \eta \leq \eta_0$, $\tilde{\varphi} < 0$ so that this equation tends to behave as

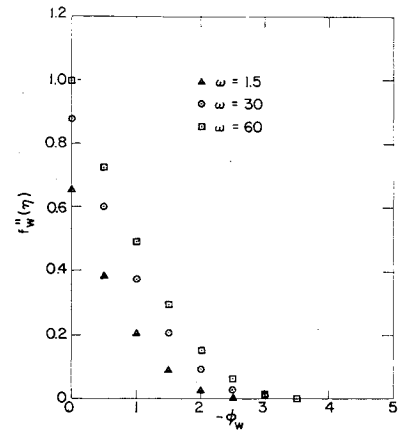

Fig. 2 Variation of streamwise shear parameter with mass transfer, $\gamma^2 = 0.3$.

$y' = Ay$, $A \gg 1$, and therefore to exhibit the sensitivity to initial data and to error growth associated with such equations. In the course of determining one iterate in the quasilinear technique, a particular solution is computed with initial data at $\eta = 0$ given by the previous iterate. Because of the behavior described previously, this particular solution cannot be found free of exponentially growing, complimentary solutions, by standard means and convergence is not achieved.

However, for the cases with $\gamma^2 = 0.3$, a value of $(-\varphi_w)$ of three is sufficient for the numerical solutions to demonstrate satisfactory agreement with the asymptotic solutions, agreement which would improve as $(-\varphi_w)$ increases. Thus there seems to be no point in reprograming to permit numerical solutions for larger η_0 to be obtained and we have not done so.

The free-mixing solutions yielding $\hat{f}(\hat{\eta})$ and $\varphi(\hat{\eta})$ are obtained by quasilinearization. With the condition $\varphi(0) = 0$ the initial value problem in this case involves the determination of $\hat{f}'(0), \hat{f}''(0), \varphi'(0), \hat{\varphi}''(0)$ so that the four requisite conditions at $\hat{\eta} \to \pm\infty$ are satisfied. We construct for each iterate four complementary solutions and one particular solurion, for each integration from $\hat{\eta} = 0$ in the direction of increasing $\hat{\eta}$ to a suitably large $\hat{\eta}$ denoted $\hat{\eta}^*$ and in the direction of decreasing $\hat{\eta}$ to a suitably large negative $\hat{\eta}$ denoted $\hat{\eta}^{**}$. These five solutions are combined so that the "infinity" conditions are satisfied at $\hat{\eta} = \hat{\eta}^*$ and $\hat{\eta}^{**}$.

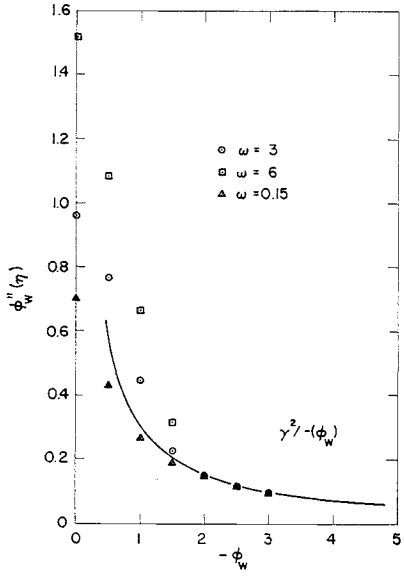

Fig. 3 Variation of chordwise shear parameter with mass transfer, $\gamma^2 = 0.3$.

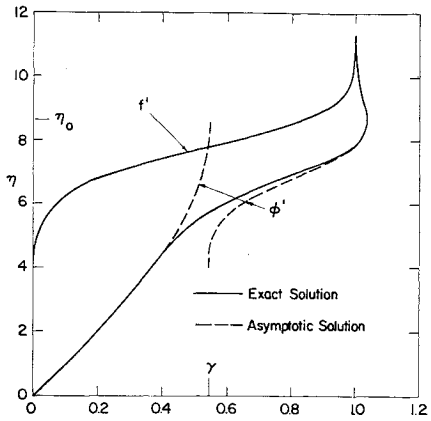

Fig. 4 Velocity profiles and comparison with asymptotic solutions; $\gamma^2 = 0.3$, $\omega = 3$ ($g_w = 0.1$), $-\delta_w = 3$.

Values of $\hat{\eta}^* = 4$, $\hat{\eta}^{**} = -6$ yield values of $|\hat{f}''(\hat{\eta})|$, $|\varphi''(\hat{\eta})|$ of 10^{-5} or less and are therefore satisfactory.

Results and Discussion

The importance of the parameter γ^2 in determining the structure of the boundary layer with large rates of injection suggests that for a given γ^2 a range of values of $(-\varphi_w)$ and of ω(or g_w) should be covered. Moreover, to provide one case in which the inner layer is more dense than the external flow and a second in which the inner layer is less dense, we take two values of γ^2, i.e., $\gamma^2 = 0.3, 3$. The related values of ω have been selected so that $g_w = 0.05, 0.1$ and 2, a range which would appear to cover most values of interest.

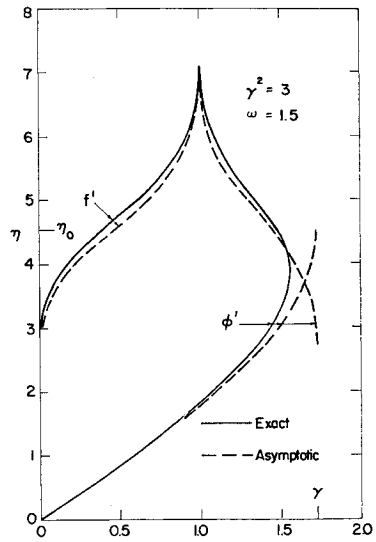

Fig. 7 Velocity profiles and comparison with asymptotic solutions; $\gamma^2 = 3$, $\omega = 1.5$ ($g_w = 2$), $-\varphi_w = 5$.

Boundary-Layer Solutions

In Table 1 we list the values of the wall shear parameters and integral thicknesses obtained from the numerical analysis. We now discuss some of the implications of these results displayed graphically.

In Figs. 2 and 3 we show for $\gamma^2 = 0.3$ the variation of the streamwise and chordwise shear parameters $f_w''(\eta)$ and $\varphi_w''(\eta)$ with $(-\varphi_w)$. Of the two variations the latter is the more interesting since we see that although for lower rates of injection $\varphi''_w(\eta)$ differs according to the value of ω (really to the value of g_w) as $(-\varphi_w)$ increases to two and beyond, $\varphi_w''(\eta)$ becomes the same and in agreement with the asymptotic expression $\varphi_w''(\eta) \sim \gamma^2/(-\varphi_w)$. Correspondingly, for $-\varphi_w \gtrsim 2, f_w''(\eta) \simeq 0$.

The excellent agreement in terms of the wall shear parameters of the asymptotic analysis and the numerical results even for relatively small values of $(-\varphi_w)$ cannot be expected to apply to the detailed structure of the boundary layer. However, at somewhat larger values of $(-\varphi_w)$ the profiles should be well predicted by the asymptotic analysis. To indicate

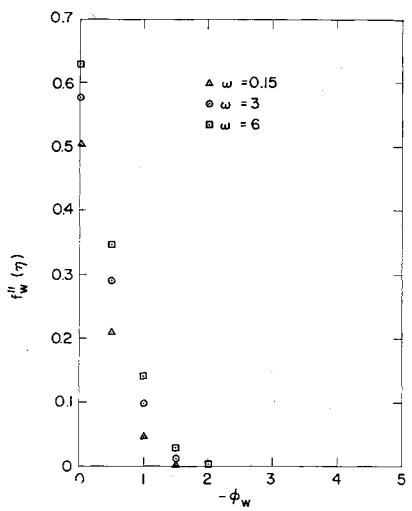

Fig. 5 Variation of streamwise shear parameter with mass transfer, $\gamma^2 = 3$.

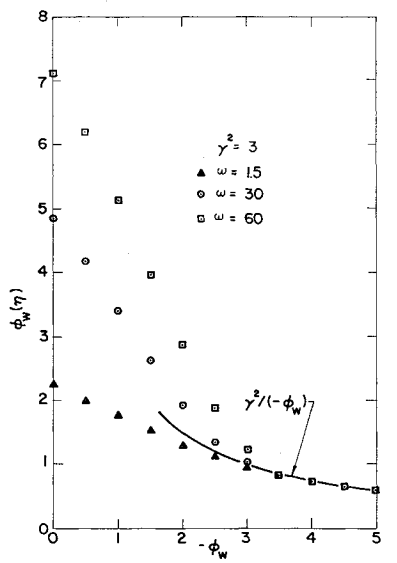

Fig. 6 Variation of chordwise parameter with mass transfer, $\gamma^2 = 3$.

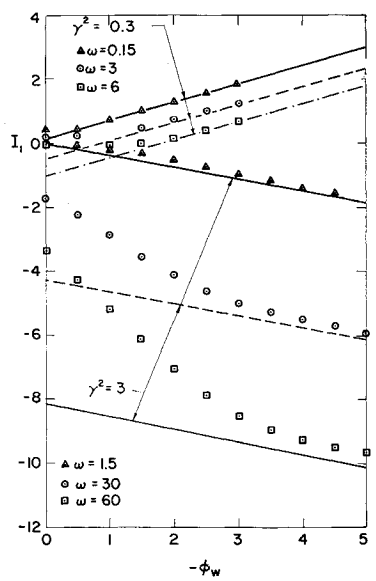

Fig. 8 Variation of integral thickness I_1 with mass transfer and comparison with asymptotic analysis.

Table 2 Properties of free-mixing solutions

γ^2	ω	$\hat{f}'(\hat{\eta}=0)$	$\hat{f}''(\hat{\eta}=0)$	$\hat{\varphi}'(\hat{\eta}=0)$	$\hat{\varphi}''(\eta=0)$	λ_1	J_1	J_2	J_3	J_4
0.3	0.15	0.5299	0.3378	0.7176	0.1660	−0.2248	0.0438	0.2195	−0.0629	−0.2731
	3	0.5196	0.3864	0.9817	0.1436	−0.9162	0.0837	−0.0457	0.4563	0.2351
	6	0.5150	0.4214	1.1955	0.1326	−1.3707	0.0184	−0.3144	0.9926	0.7615
3	1.5	0.4771	0.4746	1.4418	−0.3349	0.9977	0.0965	−0.4341	−9.3252	0.5332
	30	0.4893	0.6095	2.5482	−0.2660	−0.4056	−0.9381	−2.6552	4.0618	5.0445
	60	0.4925	0.6889	3.3268	−0.2441	−0.6951	−2.2517	−4.6563	8.0374	9.0689

this we show on Fig. 4 the velocity profiles, $f'(\eta)$, $\varphi'(\eta)$, for $\gamma^2 = 0.3, \omega = 3, (g_w = 0.1), -\varphi_w = 3$ as given by the numerical solution and by the asymptotic analysis including the free-mixing solutions for $\hat{\varphi}'(\hat{\eta})$. The difference between the exact and asymptotic solutions for $f'(\eta)$ is so small as to make impractical separate plots. It is clear that the composite profiles obtained from the asymptotic analysis give accurate approximation which can only be expected to improve as $(-\varphi_w)$ increases.

In Figs. 5–7 we show the corresponding results for $\gamma^2 = 3$, i.e., for larger sweep, low-density inner layers. Somewhat larger values of $(-\varphi_w)$ are required for the values of $f_w''(\eta)$ and $\varphi_w''(\eta)$ given by the numerical solutions to settle down to the predictions of the asymptotic analysis. The extreme case in this regard is for $\gamma^2 = 3, \omega = 60$; this requires $(-\varphi_w) \simeq 3.5$ for the wall shear parameters to be essentially those of the asymptotic analysis.

Figure 7 shows the velocity profiles for $-\varphi_w = 5$. The agreement between the exact profiles and the composite ones given by the asymptotic analysis is again seen to be excellent.

The integral thicknesses given by the exact analysis and by Eqs. (23), i.e., by the composite solutions, are shown in Figs. 8 and 9. The trends with $(-\varphi_w)$ are well predicted by the approximate analysis despite the fact that I_1, I_2 vary with $-\varphi_w$ differently for the two values of γ^2. The actual numerical values given by the exact and approximate analyses are in many cases in excellent agreement. Thus, for most purposes Eqs. (23) plus the integral thicknesses corresponding to J_i, $i = 1$–4 provide useful estimates of I_i, $i = 1, 2$ as $(-\varphi_w)$ increases.

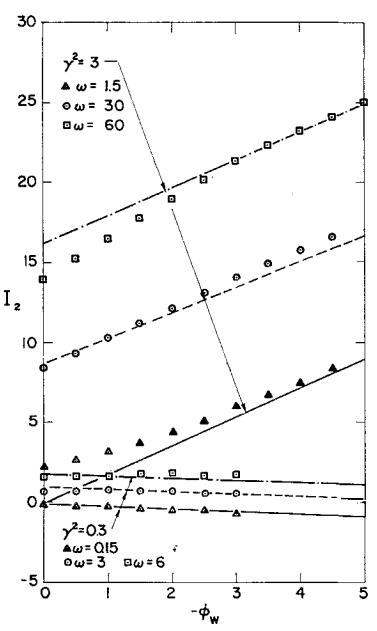

Fig. 9 Variation of integral thickness I_2 with mass transfer and comparison with asymptotic analysis.

Free-Mixing Results

In the present study the free-mixing solutions are of interest in connection with the "outer layer" behavior for large rates of injection. However, these solutions may be of interest in themselves. Accordingly, we list in Table 2 the crucial values at $\hat{\eta} = 0$, i.e., $\hat{f}'(\hat{\eta}=0), \hat{f}''(\hat{\eta}=0), \varphi'(\hat{\eta}=0), \varphi''(\hat{\eta}=0)$, the values of λ_1, and the integral thicknesses J_i, $i = 1$–4 for the pairs of γ^2, ω arising in the boundary-layer flows discussed above.

We have essentially shown in Figs. 4 and 7 the $\hat{f}'(\eta)$ and $\varphi'(\eta)$ profiles for two typical cases, one for $\gamma^2 < 1$, another for $\gamma^2 > 1$. Thus, there would appear to be no reason to indicate further examples of the profiles themselves.

References

[1] Libby, P. A., "The Homogeneous Boundary Layer at an Axisymmetric Stagnation Point with Larger Rates of Injection," *Journal of Aerospace Sciences*, Vol. 29, No. 1, Jan. 1962, pp. 48–60.

[2] Cresci, R. J. and Libby, P. A., "The Downstream Influence of Mass Transfer at the Mass of a Slender Cone," *Journal of the Aerospace Sciences*, Vol. 29, No. 7, July 1962, pp. 815–826.

[3] Aroesty, J. and Cole, J. D., "Boundary Layer Flows with Large Injection Rates," Memo RM-4620-ARPA, 1965, RAND Corp.

[4] Kassoy, D. R., "On Laminar Boundary Layer Blow Off," *SIAM Journal of Applied Mathematics*, Vol. 18, No. 1, Jan. 1970, pp. 29–40.

[5] Kubota, T. and Fernandez, F. L., "Boundary Layer Flows with Large Injection and Heat Transfer," *AIAA Journal*, Vol. 6, No. 1, Jan. 1968, pp. 22–28.

[6] Beckwith, I., "Similar Solutions for the Compressible Boundary Layer on a Yawed Cylinder with Transpiration Cooling," TR-R-42, 1959, NASA.

[7] Fox, H. and Libby, P. A., "Helium Injection into the Boundary Layer at an Axisymmetric Stagnation Point," *Journal of the Aerospace Sciences*, Vol. 29, No. 8, Aug. 1962, pp. 921–935.

[8] Radbill, J. R., "Application of Quasilinearization to Boundary-Layer Equations," *AIAA Journal*, Vol. 2, No. 10, Oct. 1964, pp. 1860–1862.

[9] Libby, P. A. and Chen, K. K., "Remarks on Quasilinearization Applied in Boundary-Layer Calculations," *AIAA Journal*, Vol. 4, No. 5, May 1968, pp. 937.